PERGAMON

Available online at www.sciencedirect.com

SCIENCE DIRECT®

Journal of Asian Earth Sciences 22 (2003) 343–352

Journal of Asian Earth Sciences

www.elsevier.com/locate/jseaes

Provenance of the Beihuaiyang lower-grade metamorphic zone of the Dabie ultrahigh-pressure collisional orogen, China: evidence from zircon ages

Fukun Chen[a,b,*], Jing-Hui Guo[a], Lai-Li Jiang[c], Wolfgang Siebel[b], Bolin Cong[a], M. Satir[b]

[a]*Key Laboratory of Mineral Resources, Institute of Geology and Geophysics, Chinese Academy of Sciences, P.O. Box 9825, Beijing 100029, People's Republic of China*

[b]*Institut für Geowissenschaften, Universität Tübingen, 72074 Tübingen, Germany*

[c]*Geological Survey of Anhui Province, Hefei 230001, People's Republic of China*

Received 22 January 2003; accepted 23 January 2003

Abstract

The Beihuaiyang zone of the Dabie ultrahigh-pressure collisional belt, which was formed by the Early Mesozoic collision of the North and South China (Yangtze) Blocks, is diversely interpreted as an active or a passive sedimentary sequence. It comprises the Luzhenguan and Foziling complexes. Six granitoid rocks of the Luzhenguan complex are dated at 770 Ma to 720 Ma and one schist sample also contains detrital zircons of 760 Ma to 720 Ma. These data indicate that this complex was of the South China affinity and probably originated from the northern Yangtze Block. Two quartzite samples of the Foziling complex contain abundant detrital zircons of Archean to Paleozoic ages, clustering around 2.5 Ga, 1.9–1.8 Ga, 1.0–0.7 Ga, and 0.5–0.4 Ga. This age spectrum demonstrates a mixed source of these two blocks. The youngest zircons suggest a Paleozoic deposition along an active continental margin south of the North China Block, while these Late Proterozoic zircons are characterized for the Yangtze Block. Subsequently, it is suggested that a terrain drifted from the northern Yangtze Block in Early Paleozoic must have been situated to the southern margin of the North China Block to provide material source prior to the final collision in Early Mesozoic.

Keywords: Dabie; Yangtze Block; North China Block; Zircon; Provenance

1. Introduction

The Dabie ultrahigh-pressure (UHP) collisional belt and its geological counterpart in the SuLu area represent the eastern part of the Qinling–Dabie orogenic belt in central China, which was formed by collision of the North China (Sino-Korean) and South China (Yangtze) Blocks during Early Mesozoic (e.g. Mattauer et al., 1985; Hsü et al., 1987; Meng and Zhang, 1999). The collision time has been constrained at about 230 Ma to 220 Ma by numerous radiometric studies (e.g. Ames et al., 1993; Li et al., 1993). Geologically, the Dabie UHP belt (Fig. 1) is made up of four major, tectonically juxtaposed zones, i.e. from south to north, the Susong high-pressure (HP) zone, the South Dabie UHP zone, the North Dabie gneiss zone (dome), and the Beihuaiyang low-grade metamorphic zone (e.g. Hacker et al., 1998). The most striking rocks are the eclogites and their host gneisses in the South Dabie UHP zone. Typical UHP metamorphic mineral inclusions are found in garnet and zircon, indicating subduction of continental crust during the collision (e.g. Liou et al., 1996; Ye et al., 2000).

Radiometric studies revealed that orthogneisses from different zones mostly have Late Proterozoic protolith ages, implying that they were derived from the South China Block (Hacker et al., 1998, 2000 and references therein). Hacker et al. (2000) have found Late Proterozoic magmatism in the Beihuaiyang zone and considered this zone as a part of the South China Block. Therefore, the suture zone between the North and South China Blocks should be located to the north of this zone. The Beihuaiyang zone that is made up of

* Corresponding author. Address: Key Laboratory of Mineral Resources, Institute of Geology and Geophysics, Chinese Academy of Sciences, P.O. Box 9825, Beijing 100029, People's Republic of China. Fax: +86-10-620-10846.

E-mail address: fukun-chen@mail.igcas.ac.cn (F. Chen).

1367-9120/03/$ - see front matter © 2003 Elsevier Ltd. All rights reserved.
doi:10.1016/S1367-9120(03)00068-3

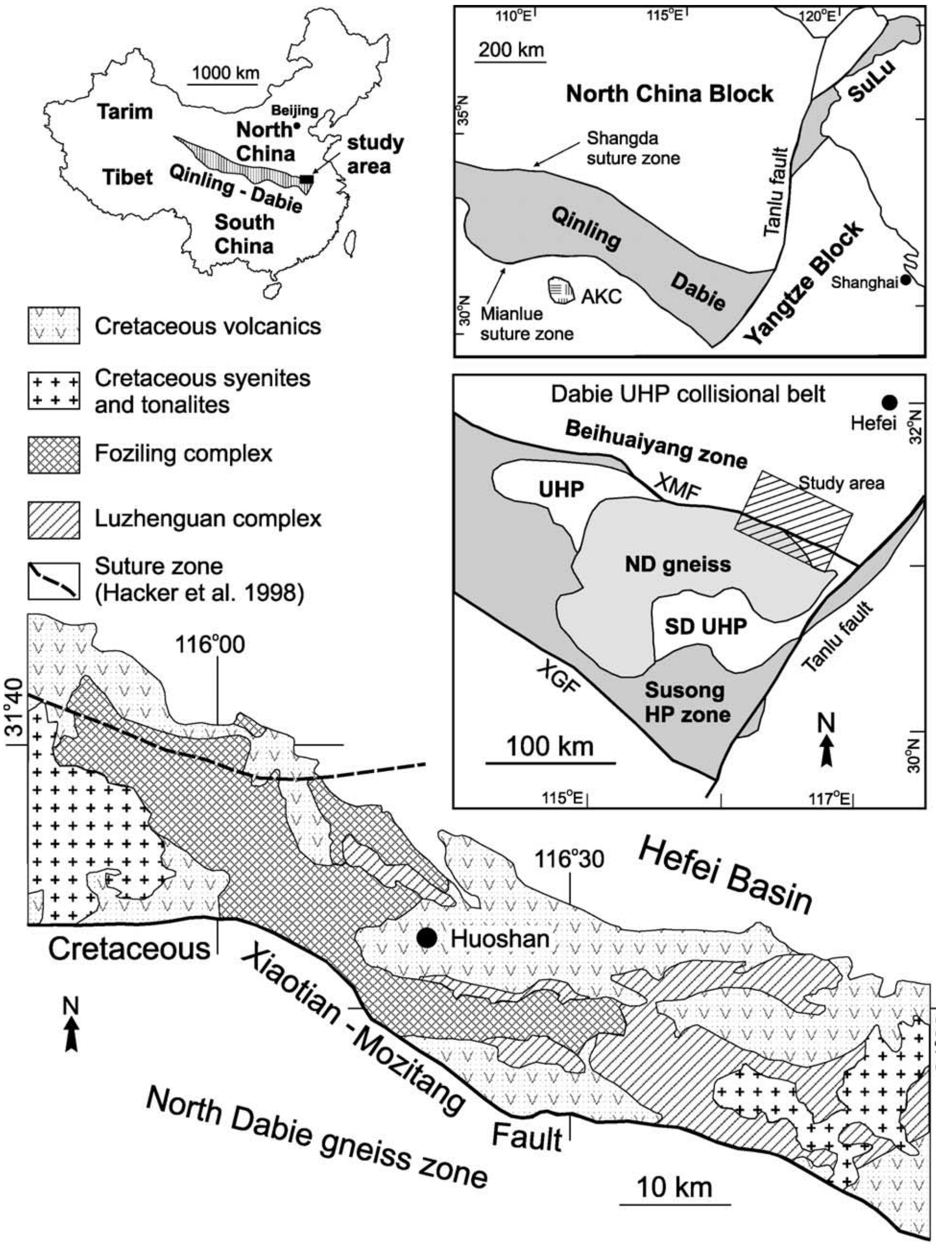

Fig. 1. Simplified geological map of the Beihuaiyang low-grade metamorphic zone in the eastern part of the Dabie UHP collisional belt (AGS, 1999; Hacker et al., 2000; Liou et al., 1995). *Abbreviations*: AKC, Archean Kongling complex; ND, North Dabie; SD, South Dabie; UHP, ultrahigh-pressure; HP, high-pressure; XMF, Xiaotian–Mozitan fault; XGF, Xiangfan–Guangji fault.

the Luzhenguan and Foziling complexes (e.g. AGS, 1999) is controversially interpreted as originating from an active or a passive continental environment. The Foziling complex is considered to be a flysch sequence that was deposited in a back-arc or fore-arc basin (e.g. Şengör et al., 1988; Dong et al., 1993). However, other investigators also favored a passive marginal environment along the northern margin of the South China Block (e.g. Okay et al., 1993; Zhou et al., 2001). This argument seems to be supported by the discovery of Late Proterozoic to Early Paleozoic microfossils in the Foziling complex and its equivalents in other parts of the Qinling–Dabie orogenic belt, which are of South China or Yangtze *sensu stricto* affinity (e.g. Zhang and Cheng, 1998). To place constraints on the origin of the Beihuaiyang zone, we have measured zircon ages of metasediments from both complexes and granitoids of the Luzhenguan complex using the U–Pb isotope dilution and Pb–Pb evaporation methods. Based on the zircon age data, we demonstrate that the Luzhenguan complex originated from the northern Yangtze Block, while the Foziling complex formed along an active margin to the southern margin of the North China Block and displays a composite source characterized by both the North and South China affinity.

2. Beihuaiyang low-grade metamorphic zone

The Beihuaiyang zone is located in the northern foot of the Dabie Mountains and is bounded by the sinistral, strike-slip Xiaotian–Mozitan fault to the North Dabie gneiss zone in south. Its northern boundary is exposed due to the Cenozoic cover of the Hefei Basin. The Beihuaiyang zone is intruded by Cretaceous syenites and tonalites and is also largely covered by Cretaceous volcanic rocks (Fig. 1). In the eastern part of this zone, it is composed of the Late Proterozoic Luzhenguan complex and Late Proterozoic to Early Paleozoic Foziling complex, which experienced greenschist- and locally up to amphibolite-facies metamorphism (e.g. AGS, 1999; Hacker et al., 1998). Comparable rock complexes occur in the western part of this orogenic belt (e.g. Okay et al., 1993) and also in the Sulu area (Zhou et al., 2002).

The Luzhenguan complex is composed of two rock units (AGS, 1999), the lower unit comprising mainly clastic-volcanic rocks and minor granitoids and amphibolites; the upper unit comprising mainly mica-quartz schist, quartzite, phyllite, and marble. The granitoids occur partly as tectonic lenses in the sediments. The Foziling complex is made up of five rock units that consist mainly of rhythmic mica-quartz schist, slate, quartz sandstone, quartzite, and minor volcanic rocks (e.g. AGS, 1999; Liou et al., 1995).

3. Analytical methods

Whole-rock powder was obtained by crushing and splitting about 10 kg of samples. Zircons were separated from the crushed rocks using a shaking table, a Frantz isodynamic separator and heavy liquids and finally handpicked under a binocular microscope. Zircon grains studied by cathodoluminescence (CL) investigation were mounted in epoxy resin and polished down to expose grain centres. The CL images were obtained using a microprobe JEOL JXA-8900RL working at 15 kV.

For Nd and Sm isotope analyses, light rare earth elements were isolated on quartz columns by conventional ion exchange chromatography with a 5 ml resin bed of AG 50W-X12 (200–400 mesh) and Sm and Nd were separated from each other and other rare-earth elements on quartz columns using 1.7 ml Teflon powder as cation exchange medium. For U–Pb analyses, single zircons or populations consisting of two to three morphologically identical grains were mechanically abraded following the Krogh (1982) method. After the abrasion, they were washed shortly in warm 7N HNO_3 and warm 6N HCl, prior to dissolution to remove surface contamination. Then, a mixed ^{205}Pb–^{235}U-tracer solution was added to the grain. Dissolution was performed in PTFE vessels in a Parr digestion bomb (Parrish, 1987) in 22N HF at 200 °C for seven days and in 6N HCl for one day to assure re-dissolution of the fluorides into chloride salts. Separation and purification of U and Pb were carried out on Teflon columns with a 40 μl bed of AG1-X8 (100–200 mesh) anion exchange resin. The technique used for single zircon Pb evaporation is that developed by Kober (1986). The Pb isotopes were dynamically measured in a sequence of 206–207–208–204–206–207 with a secondary electron multiplier. Correction of the common lead contribution to measured $^{207}Pb/^{206}Pb$ ratios followed Cocherie et al. (1992). Calculated $^{207}Pb/^{206}Pb$ ages are based on the means of all measurements evaluated and errors are given in 2σ standard deviation.

For isotopic measurements, Sm and Nd were loaded on Re-filaments and measurements were performed in a double-filament configuration. $^{143}Nd/^{144}Nd$ ratios were normalized to $^{146}Nd/^{144}Nd$ ratio of 0.7219. Analyses of the Ames metal gave a $^{143}Nd/^{144}Nd$ ratio of 0.512125 ± 0.000010 ($n = 24$), close to the reference value of 0.512147 ± 0.000007 (Roddick et al., 1992). Measured $^{143}Nd/^{144}Nd$ ratios of samples were normalized to this reference value. Pb was loaded with a Si-gel onto a Re-filament and measured at ~1300 °C in a single-filament configuration, while U was loaded with 1N HNO_3 onto a Re-filament and measured in a double-filament configuration. Total procedural Pb and U blanks were < 10 pg. A factor of 1‰ per atomic mass unit for instrumental mass fractionation was applied to all Pb analyses, using NBS 981 as reference material. Initial common Pb remaining after correction for tracer and blank was corrected using values from the Stacey and Kramers (1975) model. Analytical data were evaluated using the Pbdat and ISOPLOT programs (Ludwig, 1988, 2001) and the Wendt (1986) program. Errors are given as $2\sigma_m$. Repeated measurements on zircon standard 91500 gave nearly concordant U–Pb ages of 1065.6 ± 2.2 Ma (Chen et al., 2002), consistent with the U–Pb age of 1065.4 ± 0.3 Ma obtained in different laboratories (Wiedenbeck et al., 1995). Evaporation analyses on zircon 91500 and Phalaborwa zircon yielded $^{207}Pb/^{206}Pb$ ages of 1063 ± 5 Ma and 2054.1 ± 0.5 Ma, respectively, consistent with the reported values (Wiedenbeck et al., 1995; Kröner et al., 1993). All isotopic measurements were performed on a Finnigan MAT262 mass spectrometer. Further details on analytical techniques are given in Chen et al. (2000, 2002).

4. Analytical results

Twelve rock samples were collected from the Beihuaiyang zone, including seven granitoid and two metasediment samples of the Luzhenguan complex and three metasediment samples of the Foziling complex. Exact sample localities are given in Table 1.

4.1. Whole-rock Nd isotopic composition

Analytical results of Nd isotopic composition of the twelve whole-rock samples are given in Table 1. Seven

Table 1
Sample localities and whole-rock Nd isotopic composition of the granitoids and metasediments from the Beihuaiyang low-grade metamorphic zone

Sample no.	Rock type	Locality (Greenwich)	Sm (ppm)	Nd (ppm)	$^{147}Sm/^{144}Nd$	$^{143}Nd/^{144}Nd$ (measured)	$^{143}Nd/^{144}Nd$ (T)	$^{143}Nd/^{144}Nd$ (440 Ma)	ε_{Nd} (T)	ε_{Nd} (440 Ma)	T_{DM} (Ga)
Fuziling complex											
01HS-9	Qz-mica schist	E116°15′23″ N 31°27′51″	6.02	33.0	0.1101	0.511811	–	0.511494	–	−11.3	2.0
01HS-11	Quartzite	E116°08′25″ N 31°24′29″	2.67	13.3	0.1217	0.511944	–	0.511593	–	−9.3	1.9
01HS-12	Quartzite	E116°09′34″ N 31°26′45″	2.09	10.1	0.1256	0.511946	–	0.511584	–	−9.5	1.9
Luzhenguan complex											
01HS-13	Quartzitic schist	E116°37′24″ N 31°11′21″	3.55	18.6	0.1155	0.511757	0.511182	0.511424	−10.3	−12.6	2.1
01HS-14	Quartzitic schist	E116°38′25″ N 31°11′38″	5.48	25.0	0.1326	0.511807	0.511146	0.511425	−11.0	−12.6	2.1
00HS-15	Granite	E116°22′24″ N 31°21′54″	8.79	49.5	0.1074	0.511842	0.511307	0.511533	−6.9	−10.5	2.0
01HS-5	Granite	E116°33′21″ N 31°22′21″	5.27	29.2	0.1090	0.511644	0.511101	0.511330	−10.9	−14.5	2.3
01HS-6	Diorite	E116°37′33″ N 31°20′24″	7.11	38.6	0.1115	0.511711	0.511156	0.511390	−9.8	−13.3	2.2
01HS-7	Granite	E116°42′46″ N 31°23′17″	1.65	13.0	0.0768	0.511539	0.511177	0.511318	−10.4	−14.7	2.3
01HS-8	Granite	E116°18′03″ N 31°28′59″	11.7	70.4	0.1005	0.511816	0.511315	0.511526	−6.7	−10.6	2.0
01HS-15	Granite	E116°39′18″ N 31°11′52″	3.84	25.7	0.0903	0.511645	0.511195	0.511385	−9.0	−13.4	2.2
01HS-16	Granite	E116°40′20″ N 31°11′04″	5.22	31.5	0.1004	0.511640	0.511140	0.511350	−10.1	−14.1	2.2

1. Errors ($2\sigma_m$) of the measured $^{143}Nd/^{144}Nd$ ratios are $<1.2\times10^{-5}$. 2. Measured $^{143}Nd/^{144}Nd$ ratios were normalized to $^{146}Nd/^{144}Nd$ ratio of 0.7219. 3. Total procedure blanks are about 30 pg for Nd and about 10 pg for Sm; 4. T_{DM} values are calculated using a two-stage model for 440 Ma (Liew and Hofmann, 1988), $T = 720$ Ma for samples 01HS-13, 01HS-14, and 01HS-7; $T = 760$ Ma for samples 00HS-15, 01HS-5 to 01HS-8, 01HS-15, and 01HS-16.

granitoids of the Luzhenguan complex have initial ε_{Nd}-values of −10.9 to −6.9 (their formation ages are described below). These low ε_{Nd}-values likely indicate a substantial crustal contribution to their origin. Two schist samples of the Luzhenguan complex yield ε_{Nd}-values of −11.0 and −10.3 (calculated back to 720 Ma), while three metasediment samples of the Foziling complex have ε_{Nd}-values of −11.3 to −9.3 (calculated back to 440 Ma). Nd model ages (T_{DM}), calculated using a two-stage model of Liew and Hofmann (1988), range from 2.0 Ga to 1.9 Ga for the Foziling complex samples and from 2.3 Ga to 2.0 Ga for the Luzhenguan complex samples. When $^{143}Nd/^{144}Nd$ ratios of all analyzed samples are calculated back to 440 Ma, it becomes clear that the sediment samples of the Foziling complex have relatively higher ε_{Nd}-values (−11.3 to −9.3) than most samples of granitoid and schist of the Luzhenguan complex (−14.7 to −10.5).

4.2. Zircon ages of granites

Zircon samples from six granite rocks of the Luzhenguan complex were analyzed by the U–Pb isotope dilution and Pb–Pb evaporation methods and analytical results are given in Tables 2 and 3. These granite rocks contain prismatic zircon grains that show oscillatory zoning typical for a magmatic origin, as demonstrated in the CL images (Fig. 2). Grains 1 and 2 shown in Fig. 2 represent typical populations. Late overprint, characterized by high CL intensity along the margin, can also be observed (grain 2). All investigated grains are free of inherited cores. Using the evaporation method, four zircon grains of sample 01HS-5 were dated at 760 ± 1 Ma (Fig. 3(a)). Thirty-six analyzed fractions of zircon were analyzed for the other five granite rocks (01HS-7, 01HS-8, 00HS-15, 01HS-15, and 01HS-16) by the isotope dilution method. About 40% of them give concordant or nearly concordant U–Pb ages around 750 Ma to 720 Ma (Fig. 3(b)–(f)). When a forced regression through 220 ± 10 Ma is considered, analytical results of these five samples yield upper-intercept model ages between 766 Ma and 719 Ma, similar to a U–Pb age of 739 Ma reported for a granite from the Luzhenguan complex (Hacker et al., 2000).

4.3. Zircon ages of metasediments

Forty-two zircon grains from two quartzite samples (01HS-11 and 01HS-12) of the Foziling complex and one quartzitic schist sample (01HS-13) of the Luzhenguan complex were stepwise evaporated and measured for $^{207}Pb/^{206}Pb$ ratios. Analytical results and corresponding $^{207}Pb/^{206}Pb$ ages are given in Table 3. Zircon grains of these metasediment samples are rounded to different extents, probably indicating different sources and

Table 2
U–Pb zircon data of five granites of the Luzhenguan complex

Sample	$^{206}Pb/^{204}Pb$	U (ppm)	Pb* (ppm)	Atomic ratios				Apparent ages (Ma)		
				$^{208}Pb^*/^{206}Pb^*$	$^{206}Pb^*/^{238}U$	$^{207}Pb^*/^{235}U$	$^{207}Pb^*/^{206}Pb^*$	$^{206}Pb^*/^{238}U$	$^{207}Pb^*/^{235}U$	$^{207}Pb^*/^{206}Pb^*$
00HS-15	Granite									
(1) Long	1544	303	34.4	0.22	0.1029 ± 21	0.8968 ± 186	0.06323 ± 10	631.2	650.0	715.9
(2) Long	1421	295	36.0	0.26	0.1072 ± 22	0.9426 ± 190	0.06376 ± 9	656.6	674.3	733.8
(3) Thick	2475	295	36.4	0.25	0.1091 ± 22	0.9562 ± 194	0.06357 ± 7	667.5	681.3	727.2
(4) Thick	1714	250	28.8	0.24	0.1034 ± 21	0.9028 ± 182	0.06333 ± 7	634.2	653.2	719.3
(5) Short	725	201	24.3	0.25	0.1077 ± 22	0.9497 ± 193	0.06397 ± 14	659.3	678.0	740.5
(6) Short, fine	476	274	33.2	0.26	0.1068 ± 22	0.9418 ± 193	0.06395 ± 22	654.2	673.8	739.9
(7) Short, fine	792	278	31.0	0.24	0.1000 ± 20	0.8672 ± 176	0.06291 ± 14	614.2	634.0	705.3
(8) Long, fine	1157	324	39.0	0.24	0.1072 ± 22	0.9403 ± 190	0.06364 ± 14	656.2	673.0	729.7
(9) Long, thin	1478	226	26.6	0.28	0.1021 ± 21	0.8856 ± 181	0.06291 ± 15	626.6	644.0	705.3
(10) Long, thin	2748	401	47.4	0.27	0.1035 ± 21	0.8991 ± 182	0.06300 ± 7	634.9	651.3	708.3
01HS-7	Granite									
(11) Big, thick	483	209	28.9	0.31	0.1171 ± 24	1.0180 ± 222	0.06304 ± 35	714.0	712.9	709.6
(12) Thick	395	257	28.2	0.27	0.1173 ± 24	1.0237 ± 216	0.06330 ± 27	715.0	715.8	718.3
(13) Thick	631	332	41.2	0.22	0.1133 ± 22	0.9897 ± 201	0.06334 ± 16	692.0	698.6	719.7
(14) Short	746	211	27.5	0.25	0.1155 ± 24	1.0104 ± 210	0.06342 ± 17	704.8	709.1	722.4
(15) Long	417	303	34.2	0.21	0.1036 ± 21	0.8838 ± 185	0.06188 ± 27	635.4	643.0	669.9
(16) Long	1162	402	53.4	0.25	0.1175 ± 24	1.0190 ± 208	0.06290 ± 11	716.1	713.4	704.9
(17) Long, fine	521	354	42.0	0.26	0.1046 ± 21	0.9082 ± 185	0.06296 ± 19	641.4	656.1	707.1
(18) Long	830	322	43.0	0.25	0.1178 ± 24	1.0315 ± 209	0.06348 ± 14	718.1	719.7	724.4
01HS-8	Granite									
(19) Thick	3308	496	54.3	0.17	0.1033 ± 21	0.9056 ± 182	0.06355 ± 4	634.0	654.7	726.8
(20) Thick	4392	370	40.4	0.18	0.1024 ± 20	0.8949 ± 180	0.06338 ± 4	628.5	649.0	721.0
(21) Long	708	322	31.8	0.27	0.0859 ± 18	0.7510 ± 270	0.06339 ± 175	531.4	568.8	721.2
(22) Long	409	343	33.2	0.23	0.0874 ± 18	0.7476 ± 153	0.06202 ± 24	540.3	566.8	674.8
(23) Long, fine	1169	278	27.6	0.19	0.0920 ± 18	0.7985 ± 160	0.06296 ± 9	567.2	596.0	707.0
(24) Short	3230	372	40.3	0.20	0.0996 ± 20	0.8703 ± 174	0.06336 ± 5	612.2	635.8	720.4
01HS-15	Granite									
(25) Big, thick	1584	200	29.2	0.35	0.1187 ± 24	1.0397 ± 213	0.06354 ± 16	723.0	723.8	726.3
(26) Big, thick	4145	182	28.1	0.35	0.1273 ± 26	1.1272 ± 227	0.06421 ± 6	772.5	766.4	748.6
(27) Thick	2105	230	31.4	0.32	0.1151 ± 23	1.0243 ± 207	0.06455 ± 7	702.2	716.1	759.8
(28) Big, long	3262	208	30.4	0.35	0.1206 ± 24	1.0659 ± 214	0.06412 ± 7	733.8	736.7	745.7
(29) Long	2718	184	26.5	0.33	0.1201 ± 24	1.0590 ± 214	0.06396 ± 9	731.1	733.4	740.2
(30) Long, thin	2008	191	28.0	0.39	0.1175 ± 24	1.0318 ± 208	0.06368 ± 12	716.2	719.8	731.2
(31) Long, thin	2188	184	27.2	0.37	0.1203 ± 24	1.0561 ± 214	0.06366 ± 12	732.4	731.9	730.3
01HS-16	Granite									
(32) Long	5319	552	74.2	0.25	0.1185 ± 24	1.0513 ± 211	0.06432 ± 4	722.2	729.5	752.2
(33) Long	2138	380	46.3	0.24	0.1088 ± 22	0.9580 ± 193	0.06389 ± 8	665.5	682.3	738.0
(34) Long, thin	5633	421	56.9	0.24	0.1201 ± 24	1.0600 ± 213	0.06401 ± 5	731.1	733.8	742.1
(35) Long, thin	4890	430	57.4	0.23	0.1198 ± 24	1.0612 ± 214	0.06426 ± 6	729.2	734.4	750.3
(36) Fine	4730	403	54.6	0.28	0.1176 ± 24	1.0400 ± 209	0.06416 ± 7	716.5	723.9	746.9

1. All errors are given as $2\sigma_m$. 2. The $^{206}Pb/^{204}Pb$ ratios are measured values. 3. Concentrations of U and Pb were calculated with an estimated zircon weight. 4. Calculations of the measured U–Pb data were done using the Pbdat program (Ludwig, 1988) using 2σ errors. 5. Total procedural Pb and U blanks were about <10 pg and <5 pg during the analysis.

transport distances. Different internal structures of the investigated grains shown by CL images (Fig. 2; grains 3–6) demonstrate that each grain has an individual history. The $^{207}Pb^*/^{206}Pb^*$ ages of the forty-two zircon grains from three metasediment samples shown in Fig. 4 demonstrate that these detrital zircons have a broad age spectra between Early Archean and Early Paleozoic. At least four age peaks (2.5 Ga, 1.9 Ga to 1.8 Ga, 1.0 Ga to 0.7 Ga, and 0.5 Ga to 0.4 Ga) are distinguishable from this age spectrum. Only Proterozoic zircon ages were detected in the schist sample of the Luzhenguan complex, while two quartzite samples of the Foziling complex contain detrital zircons of Archean (up to 3.7 Ga), Proterozoic, and Paleozoic ages. The youngest zircon ages measured suggest maximum depositional ages of about 440 Ma for the Foziling complex quartzites and of about 720 Ma for the Luzhenguan complex schist, consistent with the stratigraphic sequence.

Table 3
Analytical data of single zircon grains from four samples of the Beihuaiyang lower-grade metamorphic zone, obtained by the evaporation method

Grain no.	Number of scan	$^{207}Pb^*/^{206}Pb^*$	$^{207}Pb^*/^{206}Pb^*$ age (Ma)	$^{208}Pb/^{206}Pb$ (average)	Th/U
01HS-5	Granite				
1	228	0.06451 ± 8	758 ± 3	0.22	0.70
2	190	0.06460 ± 6	761 ± 2	0.23	0.76
3	380	0.06461 ± 6	762 ± 2	0.24	0.77
4	265	0.06463 ± 5	762 ± 2	0.25	0.81
	Mean	**0.06457 ± 3**	**760 ± 1**		
01HS-13	Quartzitic schist				
1	114	0.11252 ± 22	1840 ± 4	0.08	0.27
2	114	0.11705 ± 20	1912 ± 4	0.25	0.83
3	190	0.06376 ± 14	734 ± 5	0.51	1.66
4	38	0.06410 ± 42	745 ± 14	0.63	1.98
5	114	0.06457 ± 10	760 ± 3	0.47	1.53
6	38	0.06344 ± 30	723 ± 10	0.57	1.87
7	114	0.09261 ± 20	1480 ± 5	0.26	0.87
01HS-11	Quartzite				
1	228	0.08465 ± 14	1308 ± 3	0.10	0.33
2	38	0.05606 ± 19	455 ± 8	0.17	0.52
3	38	0.15510 ± 130	2403 ± 14	0.10	0.37
4	38	0.36314 ± 6	3763 ± 2	0.03	0.12
5	300	0.06669 ± 8	828 ± 3	0.13	0.42
6	142	0.07185 ± 10	982 ± 3	0.28	0.92
7	76	0.11110 ± 28	1818 ± 5	0.14	0.46
8	228	0.06525 ± 8	782 ± 3	0.17	0.56
9	76	0.09525 ± 25	1533 ± 5	0.22	0.76
01HS-12	Quartzite				
1	304	0.16199 ± 7	2476 ± 1	0.20	0.73
2	152	0.16212 ± 15	2478 ± 2	0.22	0.79
3	76	0.09432 ± 17	1514 ± 3	0.17	0.58
4	114	0.06591 ± 17	804 ± 5	0.21	0.64
5	143	0.08229 ± 9	1252 ± 2	0.11	0.37
6	38	0.06609 ± 13	809 ± 4	0.15	0.50
7	190	0.20068 ± 14	2832 ± 1	0.21	0.75
8	190	0.05908 ± 13	570 ± 5	0.44	1.42
9	152	0.13198 ± 26	2124 ± 3	0.38	1.35
10	190	0.11693 ± 18	1910 ± 3	0.27	0.94
11	266	0.11308 ± 9	1850 ± 1	0.10	0.36
12	114	0.09057 ± 19	1438 ± 4	0.26	0.89
13	152	0.07106 ± 10	959 ± 3	0.41	1.34
14	228	0.17728 ± 7	2628 ± 1	0.07	0.06
15	266	0.06593 ± 6	804 ± 2	0.17	0.54
16	190	0.06902 ± 7	899 ± 5	0.14	0.47
17	114	0.07446 ± 17	1054 ± 4	0.05	0.14
18	114	0.11092 ± 18	1814 ± 3	0.17	0.56
19	304	0.06807 ± 5	871 ± 2	0.09	0.30
20	114	0.05562 ± 6	437 ± 3	0.18	0.56
21	266	0.06591 ± 8	803 ± 2	0.16	0.51
22	228	0.07116 ± 4	962 ± 1	0.03	0.11
23	228	0.055741 ± 9	442 ± 3	0.29	0.91
24	266	0.05725 ± 10	501 ± 4	0.04	0.10
25	228	0.11841 ± 24	1932 ± 4	0.19	0.67
26	152	0.06469 ± 20	764 ± 7	0.16	0.51

5. Discussion

Zircon geochronology using the isotope dilution, SHRIMP, and stepwise evaporation methods has been widely applied to study provenances of geologic terrains, depositional ages, and sources of sediments (e.g. Nelson, 2001; Valverde et al., 2000). Provenance of the Beihuaiyang low-grade metamorphic zone and its tectonic implications to the Qinling–Dabie orogenic belt are disputed, especially for the Foziling complex. This complex was interpreted as a flysch sequence deposited in a back-arc or fore-arc basin (e.g. Şengör et al., 1988;

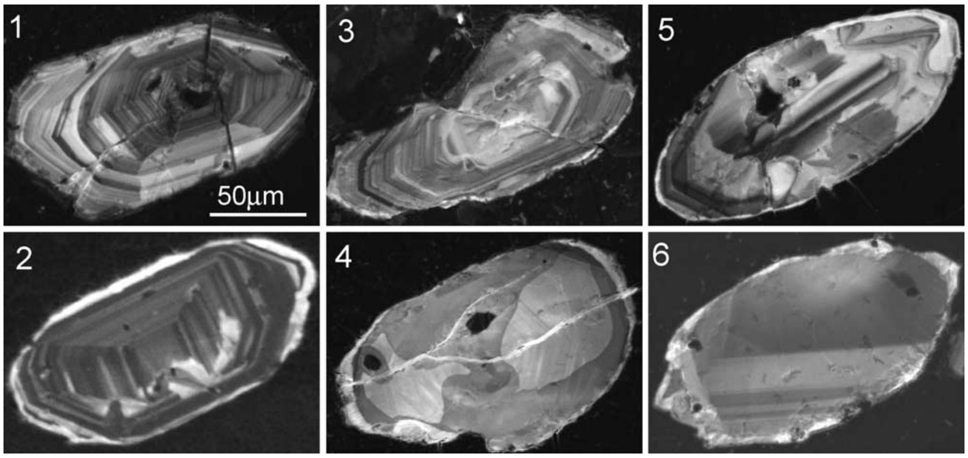

Fig. 2. Cathodoluminescence (CL) images of typical zircon populations. Grains 1 and 2 come from the Luzhenguan granitoids. They display CL oscillatory zoning typical for a magmatic origin. Late overprint characterized by the high CL intensity can be observed in the margin of Grain 2. Grains 3–6 represent major groups of detrital zircon from the Luzhenguan and Foziling sediments. Magmatic CL oscillatory zoning is well preserved in Grain 3 and recrystallization can be seen in other grains.

Dong et al., 1993) or a passive marginal sequence along the northern Yangtze Block (e.g. Okay et al., 1993; Zhou et al., 2001, 2002). The latter argument is supported by microfossils of Yangtze affinity found in the Foziling complex and its equivalents in other parts of the Qinling–Dabie orogenic belt (e.g. Zhang and Cheng, 1998). It is well known that the basements of the North and South China Blocks have had very different thermal-magmatic histories before these two blocks finally came together in Early Mesozoic (e.g. Yang et al., 1986; Ma and Bai, 1998). The North China Block is typically characterized by Archean to Early Proterozoic basement. Commonly accepted, the basement has been subjected to four major orogenic cycles during 3.0 Ga to 2.9 Ga (Qianxian cycle), 2.6 Ga to 2.5 Ga (Fupingian cycle), 2.4 Ga to 2.3 Ga (Wutaian cycle), and 1.8 Ga to 1.7 Ga (Lüliangian-Zhongyuean cycle). Although there are small Archean to Early Proterozoic basement outcrops along the north-western and western margins, e.g. the Archean Kongling complex (Gao et al., 2001), the South China Block, especially the Yangtze Block, is characterized mostly by young basement of Middle to Late Proterozoic age that became stable during the Late Proterozoic (~0.8 Ga). This young basement was subjected to major thermal-magmatic events during the Sibaon (1.1–1.0 Ga) and Jinningian–Chengjiangian (0.8–0.7 Ga) orogenic cycles. This difference allows us to put constraints on the provenance of the Beihuaiyang zone and to distinguish material sources using zircon ages.

Late Proterozoic granitoids within the Luzhenguan complex probably represent the same magmatic event that can be found in the northern and northwestern periphery of the South China Block (e.g. Rowley et al., 1997; Ames et al., 1996; Xue et al., 1997; Hacker et al., 1998; Chen et al., 2003). The quartzitic schist (01HS-13) contains many Late Proterozoic zircons (ca. 760 Ma to 720 Ma), suggesting that the 760 Ma to 720 Ma old granitoids provided material at least for part of the sediments of the Luzhenguan complex and their depositional ages should be younger than 720 Ma. When the Luzhenguan complex was drifted from the Yangtze Block and how it came to the present position remain to be answered nevertheless.

Recent studies in the Qinling region, western part of the Qinling–Dabie orogenic belt, have found that the North Qinling zone is of the North China affinity, while the South Qinling zone is favored to represent the northern margin of the South China Block (e.g. Meng and Zhang, 1999, 2000). Consequently, the Shangdan suture zone between the North and South Qinling zones, represented by an ophiolitic complex, is commonly regarded as the boundary of the North and South China Blocks (e.g. Mattauer et al., 1985; Hsü et al., 1987). Along the southern margin of the South Qinling zone, another ophiolitic complex has been also recognized, termed the Mianlue suture zone (Zhang et al., 1995). Based on this discovery, a two-stage-collision model is proposed for this orogenic belt (Meng and Zhang, 1999, 2000). According to these authors, the Shangdan suture zone was created by collision of the South and North Qinling zones during Middle Paleozoic, whereas the Mianlue suture zone resulted from the collision of the South China (Yangtze) Block and the South Qinling zone during Early Mesozoic. The South Qinling zone was separated from the South China Block during Middle Paleozoic.

Detrital zircon grains from two quartzites of the Foziling complex (01HS-11 and 01HS-12) of about 1.0 Ga to 0.7 Ga undoubtedly can be inferred as originating from a source of the South China affinity. Nevertheless, these about 500 Ma to 440 Ma old detrital zircons not only indicate a depositional age of maximum Middle Paleozoic, but also favor an active marginal

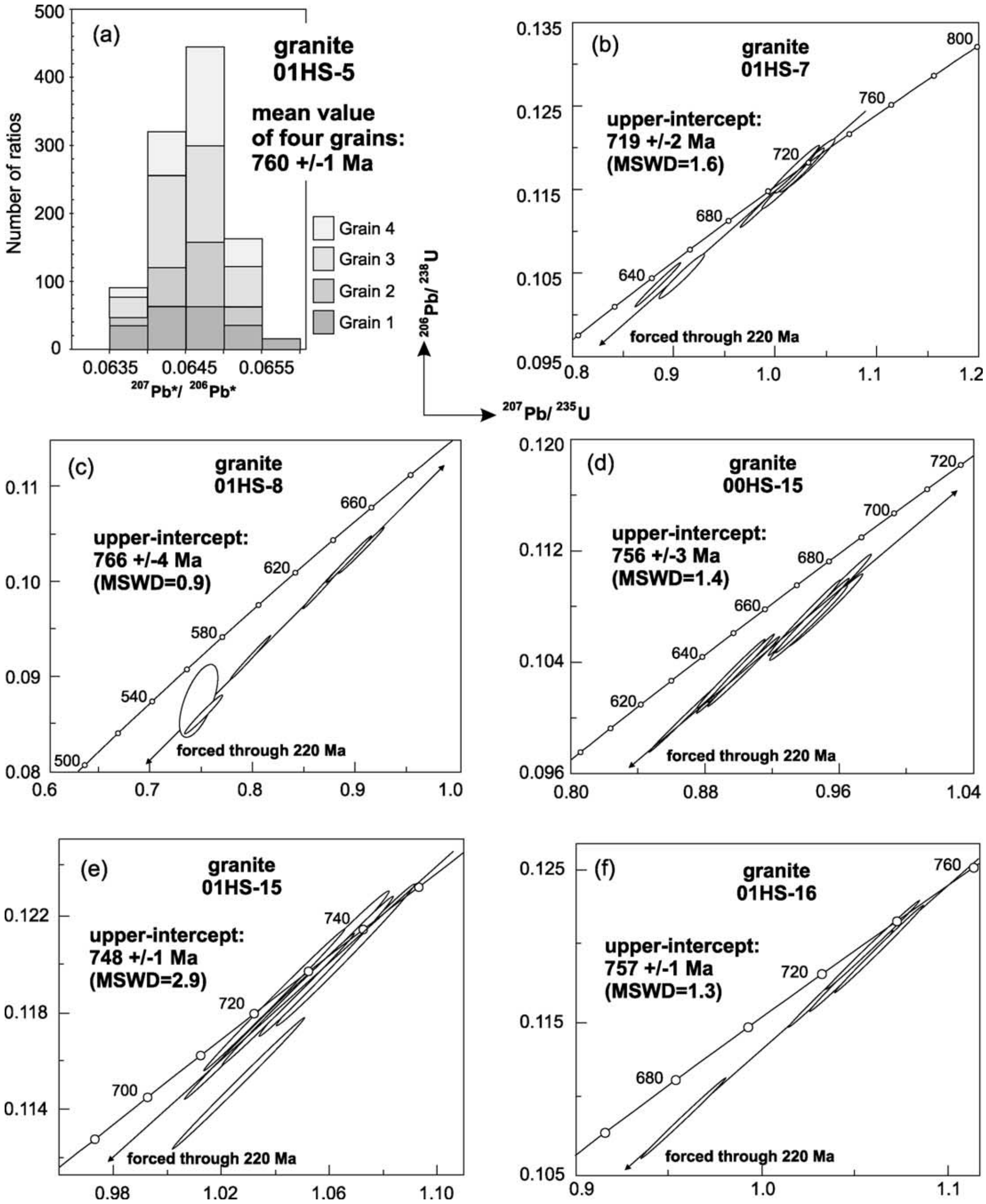

Fig. 3. Zircon ages of six granitoids from the Luzhenguan complex. (a): Histogram of $^{207}Pb^*/^{206}Pb^*$ ratios of sample 01HS-5 obtained by the evaporation method. (b)–(f): Concordia diagrams showing the U–Pb analytical results of samples 01HS-7, 01HS-8, 00HS-15, 01HS-15, and 01HS-16.

environment for the flysch sequence of the Foziling complex. The latter is indicated from the evidence that Paleozoic magmatism and metamorphism are discovered in the Shangdan or northern suture zone of the boundary of the South and North Qinling zones (e.g. Kröner et al., 1993; Zhang et al., 1997), which represents the collision of these two zones during the Middle Paleozoic (e.g. Meng and Zhang, 1999, 2000). The metasediment samples of the Foziling complex roughly display higher ε_{Nd}-values than granitoids and metasediments of the Luzhenguan complex of this study as well as gneisses from the South China Block (Chen and Jahn, 1998; Ma et al., 2000). This Nd isotopic signature can imply involvement of material from young magmatic rocks of an active continental margin. In this context, we consider the basement of the North China Block as a possible source for these Archean and Early Proterozoic detrital zircons (two age peaks of 2.5 Ga and 1.8 Ga) of the Foziling complex.

In summary, detrital zircon ages combined with Nd isotopic composition of the Foziling complex are considered as supporting an active North China other than a passive South China continental margin as a deposit setting for the Foziling flysch sequence. Nevertheless,

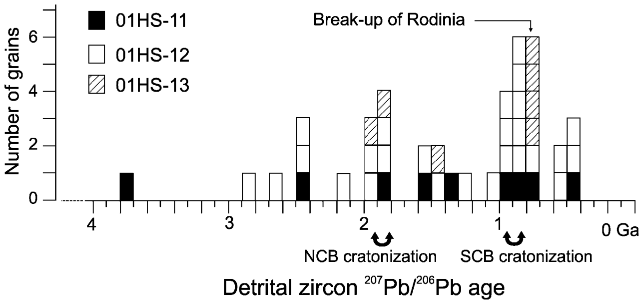

Fig. 4. A $^{207}Pb^*/^{206}Pb^*$ age spectra outlined for detrital zircons of a Luzhenguan schist (01HS-13) and two Foziling quartzites (01HS-11 and 01HS-12). At least four age peaks at ca. 2.5 Ga, 1.9–1.8 Ga, 0.9–0.7 Ga, and 0.5–0.4 Ga can be observed. NCB: North China Block; SCB: South China Block.

a tectonic setting has to be found that allow the Paleozoic Foziling flysch to become a source of material that portrays both characteristics of basement rocks from the active and passive continents, i.e. from both the North and South China Blocks. The discovery of the Mianlue suture zone in the southern margin of the South Qinling zone (Zhang et al., 1995) and the two-stage collisional model of the Qinling–Dabie orogenic belt (Meng and Zhang, 1999, 2000) provide a tectonic framework to better understand the detrital zircon provenance and the origin of the Foziling complex (Fig. 5). The South Qinling zone of the South China affinity might be the source for the Late Proterozoic (about 1.0 Ga to 0.7 Ga) as well as Middle Proterozoic (about 1.6 Ga to 1.2 Ga) detrital zircons of the Foziling complex. Late Proterozoic magmatic zircons from granitoids and detrital zircons from metasediements found in the Luzhenguan complex indicate an origin from the South China (Yangtze) Block. Similar zircon ages have been frequently reported for other metamorphic zones in the Dabie UHP collisional belt (e.g. Rowley et al., 1997; Ames et al., 1996; Hacker et al., 1998, 2000; Xue et al., 1997; Chen et al., 2003). On the basis of the zircon age data, we consider that the Luzhenguan complex was derived from the northern margin of the Yangtze Block, probably simultaneously with the South Qinling zone or is part of the basement of this zone.

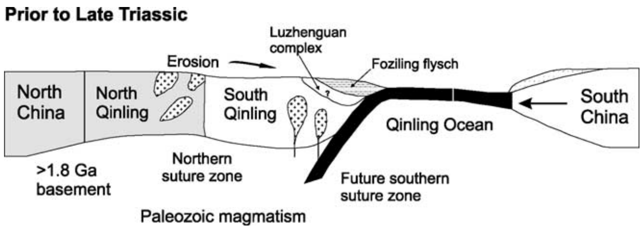

Fig. 5. A sketch diagram shows the depositional environment and source of the Foziling complex prior to the final collision of the North and South China Blocks in Early Mesozoic. The tectonic framework follows a two-stage collisional model for the Qinling–Dabie orogenic belt proposed by Meng and Zhang, 1999, 2000).

6. Conclusions

The Beihuaiyang lower-grade metamorphic zone of the Dabie UHP collisional belt is made up of two rock complexes of different provenances. The Luzhenguan complex prominently comprises numerous granitoids rock forming in Late Proterozoic (about 760 Ma to 720 Ma), clearly indicating an origin of the northern margin of the South China (Yangtze) Block. The flysch sequence of the Foziling complex characteristically contains Late Proterozoic and Paleozoic detrital zircons that originated from two different material sources, the first ones from the passive Yangtze Block and the latter ones from the active continental margin south to the North China Block. Based on these results, it is proposed that the Luzhenguan complex, like the South Qinling zone, was probably located to south of the North China Block before the collision of the North and South China Blocks in Early Mesozoic. Consequently, the flysch sequence became material sources characterized by the mixed feature of these two continental blocks during the Paleozoic deposition.

Acknowledgements

This study was supported by the Ministry of Science and Technology of China within the priority program “Deep Subduction of Continents” (G1999075502) and National Natural Science Foundation of China (NSFC; 40072070) and resulted from the cooperative project between University of Tübingen and Chinese Academy of Sciences. Sincere thanks are due to Y.-F. Zheng for discussion, to T. Vennemann for English improvement, and to P. E. Buchholz and an anonymous reviewer for comments on the manuscript.

References

Ames, L., Tilton, G.R., Zhou, G., 1993. Timing of collision of the Sino-Korean and Yangtze cratons: U–Pb zircon dating of coesite-bearing eclogites. Geology 21, 339–342.

Ames, L., Zhou, G.-Z., Xiong, B.-C., 1996. Geochronology and isotopic character of ultrahigh pressure metamorphism with implications for collision of the Sino-Korean and Yangtze cartons, central China. Tectonics 15, 472–489.

Anhui Geological Survey, 1999. Explanation of the 1:250000 geological map of the Dabie Mountains within Anhui Province. Anhui Geol. Surv. Hefei, 44in Chinese.

Chen, J., Jahn, B., 1998. Crustal evolution of southeastern China: Nd and Sr isotopic evidence. Tectonophysics 284, 101–133.

Chen, F., Hegner, E., Todt, W., 2000. Zircon ages and Nd isotopic and chemical compositions of orthogneisses from the Black forest, Germany: evidence for a Cambrian magmatic arc. Int. J. Earth Sci. 88, 791–802.

Chen, F., Siebel, W., Satir, M., 2002. Zircon U–Pb and Pb-isotope fractionation during stepwise HF-acid leaching and geochronological implications. Chem. Geol. 191, 153–162.

Chen, F., Siebel, W., Guo, J.-H., Cong, B., Satir, M., 2003. Late Proterozoic magmatism and metamorphism recorded in gneisses from the Dabie high-pressure metamorphic zone, eastern China: evidence from zircon U–Pb geochronology. Precamb. Res. 120, 131–148.

Cocherie, A., Guerrot, C., Rossi, P.H., 1992. Single-zircon dating by step-wise Pb evaporation: Comparison with other geochronological techniques applied to the Hercynian granites of Corsica. France Chem. Geol. 101, 131–141.

Dong, S., Sun, S., Zhang, Y., Huang, D., Wang, G., Dai, S., 1993. Fundamental structure of the Dabieshan collision-type orogenic belt. Chinese Sci. Bull. 38, 542–545.

Gao, S., Qiu, Y., Ling, W., McNaughton, N.J., Groves, D.I., 2001. Single zircon SHRIMP U–Pb geochronology of the Kongling high-grade metamorphic terrain—a discovery of >3.2 Ga crustal material in the Yangtze craton. Sci. China (D) 31, 27–35.in Chinese.

Hacker, B.R., Ratschbacher, L., Webb, L., Ireland, T., Walker, D., Dong, S., 1998. U/Pb zircon ages constrain the architecture of the ultrahigh-pressure Qinling–Dabie orogen, China. Earth Planet Sci. Lett. 161, 215–230.

Hacker, B.R., Ratschbacher, L., Webb, L., McWilliams, M.O., Ireland, T., Calvert, A., Dong, S., Wenk, H.-R., Chateigner, D., 2000. Exhumation of ultrahigh-pressure continental crust in east central China: Late Triassic—Early Jurassic tectonic unroofing. J. Geophys. Res. 105 (B6), 13339–13364.

Hsü, K.J., Wang, Q., Li, J., Zhou, D., Sun, S., 1987. Tectonic evolution of Qinling Mountains, China. Eclogae Geolog. Helvetiae 80, 735–752.

Kober, B., 1986. Whole-grain evaporation for $^{207}Pb/^{206}Pb$ age investigations on single zircons using a double-filament thermal ion source. Contrib. Mineral. Petrol. 93, 481–490.

Kröner, A., Zhang, G., Sun, Y., 1993. Granulites in the Tongbai area, Qinling belt, China: Geochemistry, petrology, single zircon geochronology, and implications for the tectonic evolution of eastern Asia. Tectonics 12, 245–255.

Krogh, T.E., 1982. Improved accuracy of U–Pb zircon ages by the creation of more concordant systems using an air abrasion technique. Geochim. Cosmochim. Acta 46, 637–649.

Li, S.-G., Xiao, Y., Liou, D., Chen, Y., Ge, N., Zhang, Z., Sun, S., Cong, B., Zhang, R., Hart, S.R., Wang, S., 1993. Collision of the North China and Yangtze blocks and formation of coesite-bearing eclogites: timing and processes. Chem. Geol. 109, 89–111.

Liew, T.C., Hofmann, A.W., 1988. Precambrian crustal components, plutonic associations, plate environment of the Hercynian Fold Belt of central Europe: Indications from a Nd and Sr isotopic study. Contrib. Mineral. Petrol. 98, 129–138.

Liou, J.-G., Wang, Q.-C., Zhai, M.-G., Zhang, R.-Y., Cong, B.-L., 1995. Ultrahigh-P metamorphic rocks and their associated lithologies from the Dabie terrain, Central China: a field trip guide to the 3rd international eclogite field symposium. Chinese Sci. Bull. 40 (Suppl.), 1–40.

Liou, J.G., Zhang, R.Y., Eide, E.A., Maruyama, S., Wang, X., Ernst, W.G., 1996. Metamorphism and tectonics of high-P and ultrahigh-P belts in Dabie–Sulu regions, eastern central China. In: Yin, A., Harrison, T.M. (Eds.), The Tectonic Evolution of Asia, Cambridge University, New York, pp. 300–343.

Ludwig, K.R., 1988. Pbdat for MS-Dos—a computer program for IBM-PC compatibles for processing raw Pb–U–Th isotope data. US Geol. Surv., 1–37.Open-file Report 88–542.

Ludwig, K.R., 2001. Isoplot/Ex, rev 2.49: A Geochronological Toolkit for Microsoft Excel. Berkeley Geochron, Center Spec. Publ. No. 1a, 58p.

Ma, X.-Y., Bai, J., 1998. Precambrian Crustal Evolution of China, Springer/Geol. Publishing House, Berlin-Heidelberg/Beijing.

Ma, C.-Q., Ehlers, C., Xu, C., Li, Z., Yang, K., 2000. The roots of the Dabieshan ultrahigh-pressure metamorphic terrane: constraints from geochemistry and Nd–Sr isotope systematics. Precamb. Res. 102, 279–301.

Mattauer, M., Matte, Ph., Malavieille, J., Tapponnier, P., Maluski, H., Xu, Z., Lu, Y., Tang, Y., 1985. Tectonics of the Qinling belt: build-up and evolution of eastern Asia. Nature 317, 496–500.

Meng, Q.-R., Zhang, G., 1999. Timing of collision of the North and South China blocks: Controversy and reconciliation. Geology 27, 123–126.

Meng, Q.-R., Zhang, G., 2000. Geologic framework and tectonic evolution of the Qinling orogen, central China. Tectonophysics 323, 183–196.

Nelson, D.R., 2001. An assessment of the determination of depositional ages for Precambrian clastic sedimentary rocks by U–Pb dating of detrital zircons. Sediment. Geol., 141–142.see also pp. 37–60.

Okay, A.I., Şengör, A.M.C., Satir, M., 1993. Tectonics of an ultrahigh-pressure metamorphic terrane: the Dabie Shan–Tongbai Shan orogen, China. Tectonics 12, 1320–1334.

Parrish, R.R., 1987. An improved micro-capsule for zircon dissolution in U–Pb geochronology. Chem. Geol. 66, 99–102.

Rowley, D.B., Xue, F., Tucker, R.D., Peng, Z.-X., Baker, J., Davis, A., 1997. Ages of ultrahigh pressure metamorphism and protolith orthogneisses from the eastern Dabie Shan: U/Pb zircon geochronology. Earth Planet Sci. Lett. 151, 191–203.

Roddick, J.C., Sullivan, R.W., Dudás, F.Ö., 1992. Precise calibration of Nd tracer isotopic composition for Sm–Nd studies. Chem. Geol. 97, 1–8.

Şengör, A.M.C., Altiner, D., Cin, A., Ustaömer, T., Hsü, K.J., 1988. Origin and assembly of the Tethyside orogenic collage at the expense of Gondwana Land. Geol. Surv. Spec. Publ. London, No. 37, 119–181.

Stacey, J.S., Kramers, J.D., 1975. Approximation of terrestrial lead isotope evolution by a two stage model. Earth Planet Sci. Lett. 26, 207–221.

Valverde, V.P., Doerr, W., Belka, Z., Franke, W., Wiszniewska, J., Schastok, J., 2000. U–Pb single-grain dating of detrital zircon in the Cambrian of central Poland; implications for Gondwana versus Baltica provenance studies. Earth Planet Sci. Lett. 184, 225–240.

Wendt, I., 1986. Radiometrische Methoden in der Geochronologie, Clausthaler Tektonische Hefte 23, Pilger, p. 170.

Wiedenbeck, M., Allé, P., Corfu, F., Griffin, W.L., Meier, M., Oberli, F., von Quadt, A., Roddick, J.C., Spiegel, W., 1995. Three natural zircon standards for U–Th–Pb, Lu–Hf, trace element and REE analyses. Geostand. Newslett. 19, 1–23.

Xue, F., Rowley, D.B., Tucker, R.D., 1997. U–Pb zircon ages of granitoid rocks in the north Dabie Complex, eastern Dabie Shan, China. J. Geol. 105, 744–753.

Yang, Z.-Y., Cheng, Y.-Q., Wang, H.-Z., 1986. The geology of China. Oxford Monographs Geol. Geophys. 3 Oxford, 303.

Ye, K., Cong, B.-L., Ye, D.-N., 2000. The possible subduction of continental materials to depths greater than 200 km. Nature 407, 734–736.

Zhang, R., Cheng, X., 1998. The discovery of early Ordovician microfossils from the Sujiahe group of Tongbo–Dabie orogenic belt and its significances. Acta Micropaleont. Sinica 15, 125–133.

Zhang, G.-W., Meng, Q., Lai, S., 1995. Tectonics and structures of the Qinling orogenic belt. Sci. China (D) 38, 1379–1386.

Zhang, H.-F., Gao, S., Zhang, B., Luo, T.-C., Lin, W., 1997. Pb isotopes of granitoids suggest Devonian accretion of the Yangtze (South China) to North China cratons. Geology 25, 1015–1018.

Zhou, J.-B., Zheng, Y.-F., Li, L., Xie, Z., 2001. Accretionary wedge of the subduction of the Yangtze plate. Acta Geol. Sinica 75, 338–352.in Chinese, with English abstract.

Zhou, J.-B., Zheng, Y.-F., Wu, Y.-B., 2002. U–Pb zircon ages of the Wulian granite from the northwestern margin of the Sulu orogenic belt and geological implications. Chinese Sci. Bell. 47, 1745–1750.in Chinese.